Chemico-Biological Interactions 181 (2009) 455–462

Contents lists available at ScienceDirect

Chemico-Biological Interactions

journal homepage: www.elsevier.com/locate/chembioint

A proteomic investigation into the human cervical cancer cell line HeLa treated with dicitratoytterbium (III) complex

Liming Shen [a], Qiong Liu [a,*], Jiazuan Ni [a], Guangyan Hong [b]

[a] College of Life Sciences, Shenzhen University, Nanhai Road #3688, Nanshan District, Shenzhen 518060, Guangdong Province, PR China
[b] Changchun Institute of Applied Chemistry, Chinese Academy of Sciences, Changchun 130022, PR China

ARTICLE INFO

Article history:
Received 12 April 2009
Received in revised form 16 July 2009
Accepted 16 July 2009
Available online 24 July 2009

Keywords:
Ytterbium
Dicitratoytterbium (III) complex
HeLa cells
Proteomics
Dicitratolanthanum (III) complex

ABSTRACT

Lanthanides have been reported to induce apoptosis in cancer cell lines. Human cervical cancer cell line HeLa was found to be more sensitive to dicitratolanthanum (III) complex ($[LaCit_2]^{3-}$) than other cancer cell lines. However, the effect and mechanism of dicitratoytterbium (III) complex ($[YbCit_2]^{3-}$) on HeLa cells is unknown. Using biochemical and comparative proteomic analyses, $[YbCit_2]^{3-}$ was found to inhibit HeLa cell growth and induce apoptosis. Similar to the effects of $[LaCit_2]^{3-}$, proteomics results from $[YbCit_2]^{3-}$-treated cells revealed profound changes in proteins relating to mitochondria and oxidative stress, suggesting that mitochondrial dysfunction plays a key role in $[YbCit_2]^{3-}$-induced apoptosis. This was confirmed by the decreased mitochondrial transmembrane potential and the increased generation of reactive oxygen species in $[YbCit_2]^{3-}$-treated cells. Western blot analysis showed that $[YbCit_2]^{3-}$-induced apoptosis was accompanied by the activation of caspase-9 and specific proteolytic cleavage of PARP, leading to an increase in the pro-apoptotic protein Bax and a decrease in the anti-apoptotic protein Bcl-2. These results suggest a mitochondrial pathway of cell apoptosis in $[YbCit_2]^{3-}$-treated cells, which will help us understand the molecular mechanisms of lanthanide-induced apoptosis in tumor cells.

1. Introduction

Lanthanides (Lns) have been reported to have a variety of biological effects and potentials in medical applications. For example, gadolinium (III) compounds are widely used as diagnostic contrast agents; lanthanum carbonate has been proposed as a phosphate binder for the treatment of hyperphosphatemia in patients with chronic renal failure [1], and motexafin gadolinium is a new chemotherapeutic agent selectively targeting tumor cells which is undergoing clinical trials for the treatment of brain metastases of lung cancers [2].

Effects of Lns on cell proliferation and apoptosis have also been extensively studied [3–5], showing that the promotion of cell proliferation and induction of apoptosis depends on the species and concentration of particular Ln, cell types and selective cytotoxicity of Lns on tumor cells [5,6]. The growth of cultured B16 melanoma cells was reported to be inhibited by La^{3+}, Ce^{3+}, Nd^{3+}, Sm^{3+}, Gd^{3+} and Yb^{3+} to stop in the cell cycle of G0/G1 to S phase [7]. Additionally, it was proposed that La^{3+}, Gd^{3+} and Yb^{3+}-induced apoptosis *via* the mitochondria pathway involving reactive oxygen species (ROS) in the mechanism [8]. Our previous studies showed dose-dependent effects of dicitratolanthanum (III) complex ($[LaCit_2]^{3-}$) on the growth and viability of different cancer cell lines. The most potent cytotoxicity was observed in HeLa cells [9]. The mechanism of $[LaCit_2]^{3-}$ on HeLa cells was also investigated by comparative proteomics and the results suggested an intrinsic pathway of cell apoptosis in $[LaCit_2]^{3-}$-treated cells (unpublished).

There is a global public health burden attributable to the human papilloma virus (HPV) and the link with cervical cancer has been proven conclusively [10,11]. A recent study showed that a short treatment of cells with La^{3+}, Ce^{3+}, Pr^{3+} and Nd^{3+} changed the cellular chemistry into a state in which the RNA replication of flaviviruses was blocked specifically without interfering with host cell multiplication [12]. This raised interest about the potential inhibitory activity of Lns on the replication of HPV and its possibility to be developed as a drug for therapy in patients with cervical cancer.

Lns comprise a group of metal ions with similar properties, including the light, medium and heavy forms. As lanthanum is a light Ln, ytterbium was chosen as a representative of heavy Ln

Abbreviations: GAPDH, glyceraldehyde 3-phosphate dehydrogenase; HPV, human papillomavirus; MTT, 3-(4,5-dimethylthiazol-2-yl)-2,5-diphenyltetrazolium bromide; JC-1, 5′,6,6′-tetrachloro-1,1′,3,3′-tetraethylbenzimidazolcarbo-cyanineiodide; PTP, permeability transition pore; ROS, reactive oxygen species; $\Delta\psi_m$, mitochondrial transmembrane potential; DCFH-DA, 2′7′-dichlorofluorescein; VDAC, voltage-dependent anion-selective channel; SOD1, copper zinc superoxide dismutase 1; PHB, prohibitin; PARP, poly ADP-ribose polymerase; eIF3i, eukaryotic translation initiation factor 3, subunit 2; QPRTase, quinolinate phosphoribosyltransferase; VDAC, voltage-dependent anion-selective channel; eEF2, eukaryotic translation elongation factor 2; DTT, DL-dithiothreitol.

* Corresponding author. Tel.: +86 755 26535432; fax: +86 755 26534274.
E-mail address: liuqiong@szu.edu.cn (Q. Liu).

0009-2797/$ – see front matter © 2009 Elsevier Ireland Ltd. All rights reserved.
doi:10.1016/j.cbi.2009.07.013

forms in the present study, for the investigation of its effect and mechanism on HeLa cells.

Two-dimensional gel electrophoresis (2DE) is one of the most powerful tools in proteomics studies. It allows a fast overview of changes in cell processes through the analysis of entire protein extracts from biological and medical systems [13]. With the aids of proteomic approaches, twelve differentially expressed proteins were identified in $[YbCit_2]^{3-}$-treated HeLa cells, which were involved in cell apoptosis or proliferation, redox regulation, and protein translation or degradation. Confirmation and further investigation showed that $[YbCit_2]^{3-}$-induced apoptosis of HeLa cells *via* intrinsic pathways similar to that of $[LaCit_2]^{3-}$.

2. Materials and methods

2.1. Chemical reagents

$[YbCit_2]^{3-}$ solution was prepared from ytterbium oxide (purity >99.9%, Yuelong New Materials Co., Ltd., Shanghai, PR China) and citric acid (BBI, Canada). Ytterbium oxide was dried at 105–110 °C for 2 h and cooled down in a desiccator before being weighed accurately. A proper amount of ytterbium oxide was dissolved in 6 mol/L hydrochloric acid and heated to expel the excess amount of HCl. The obtained pellet was completely dissolved in 2.5 mol/L citric acid solution at a given amount, adjusted to pH 7.0 with NaOH and then diluted with ultrapure water to 20 mmol/L $[YbCit_2]^{3-}$ as a stock solution. All other reagents, except otherwise noted, were obtained from GE Healthcare (Yian Plaza, Guangzhou, PR China).

2.2. Cell culture

HeLa cells were obtained from the Shanghai Institute of Biochemistry and Cell Biology, Chinese Academy of Sciences. Cells were cultured in RPMI-1640 medium plus 10% fetal bovine serum (Hyclone, Logan, UT, USA), 100 U/mL penicillin and 100 μg/mL streptomycin (Merck & Co., Inc., Whitehouse Station, NJ, USA). The cells were maintained in a humidified incubator with an atmosphere of 95% air and 5% CO_2 at 37 °C. When the cells reached 80% confluence, they were harvested and plated for either subsequent passages or drug treatments. For the treated samples, complete medium was removed and fresh RPMI-1640 medium (fetal bovine serum, FBS-free) containing $[YbCit_2]^{3-}$ was added.

2.3. Cell viability assay

Cell viability was determined by MTT assay as reflected by the activity of succinate dehydrogenase [14]. HeLa cells (1×10^3 per well) were plated in 96-well microplates. On the next day, the medium was replaced with fresh medium at various concentrations of $[YbCit_2]^{3-}$ in a final volume of 200 μL. After 24 h treatment, 20 μL of 5 mg/mL MTT (Sigma–Aldrich, St Louis, MO, USA) in phosphate buffered saline (PBS) was added to each well for an additional 4 h, then the medium was removed and 150 μL DMSO (Amresco, Solon, OH, USA) was added to dissolve the MTT formazan precipitate. The absorbance of samples was measured at 570 nm with a SpecTRA MAX 190 microplate reader (Molecular Devices, Sunnyvale, CA, USA). Cells without $[YbCit_2]^{3-}$ treatment served as the control. Triplicate runs were performed throughout.

2.4. Morphological observations

To detect morphological changes during apoptosis, nuclear staining was performed with 5 μg/mL Hoechst 33258 (Beyotime Institute of Biotechnology, Jiangsu, PR China) and cells were analyzed using a fluorescence microscope (Olympus, Japan). Over 200 cells were counted for each well in triplicate.

2.5. Flow cytometric analysis of apoptosis

To assess the percentages of viable and apoptotic cells, double-staining using annexin coupled with fluorescein isothiocyanate (FITC)/propidium iodide (PI) was performed using an annexin V-FITC kit (Nanjing Institute of Jiancheng Biological Engineering, PR China). Cells were processed as described in the manufacturer's protocol and analyzed using flow cytometry.

2.6. Protein extraction

After treatment with 0.1 mmol/L $[YbCit_2]^{3-}$ for 24 h, the HeLa cells were washed with ice-cold phosphate buffered saline (PBS). The cells were harvested by treatment with 0.02% EDTA in PBS solution, washed with PBS and centrifuged at 1000 rpm for 5 min. After two washes with 1 mL of PBS, the cell pellet was lysed in lysis buffer (7 mol/L urea, 2 mol/L thiourea, 4% CHAPS, 2% pharmalyte pH 3.11, 20 mmol/L DTT and 40 mmol/L Tris base), sonicated 10 times for 5 s with 10 s pauses in an ice-water bath and centrifuged at 14,000 rpm for 60 min at 4 °C. The supernatants were used directly for gel electrophoresis. Triplicate samples were prepared independently. Cells without $[YbCit_2]^{3-}$ treatment were used as the control.

2.7. Two-dimensional gel electrophoresis (2DE)

2DE was performed with IPGphor isoelectric focusing (IEF) and electrophoresis units (GE Healthcare). Whole cell protein lysates (150 μg) were mixed with rehydration solution (8 mol/L urea, 4% CHAPS, 0.5% IPG buffer and 0.12% DeStreak Reagent) to a final volume of 450 μL. Precast 24-cm immobilized pH gradient (IPG) strips were rehydrated for 12 h at 30 V. IEF was performed in a step-and-hold pattern of 100 V for 2 h, 200 V for 1 h and 500 V for 1 h. Then a gradient pattern was used to reach 1000 V for 1 h and 8000 V for 3 h, followed by a step-and-hold pattern of 8000 V for 8 h and a holding pattern of 500 V. After the first dimensional run, the proteins were reduced (6 mol/L urea, 30% glycerol, 2% SDS and 50 mmol/L Tris–HCl, pH 6.8) and alkylated for 15 min in the same buffer containing 135 mmol/L iodoacetamide instead of DTT. Then, proteins were separated in the second dimension on homemade 12.5% SDS polyacrylamide gels using the Ettan DALTsix Electrophoresis Unit (GE Healthcare). Analytical gels were stained with silver nitrate and preparative gels were stained with CBB R-250. Gels were scanned using a ProXPRESS 2D imaging system (PerkinElmer Inc., Waltham, MA, USA) and analyzed with Image Master 2D Elite software (GE Healthcare). Data were obtained in triplicates, normalized and expressed as percentages of all valid spots to account for differences in protein loading and staining. Only those spots that changed consistently and significantly (more than 2-fold) were selected for mass spectrometry analysis.

2.8. In-gel digestion with trypsin

Protein spots differentially expressed in 2D gels were excised and destained with 50% acetonitrile and 25 mmol/L ammonium bicarbonate. After dehydrating with acetonitrile and drying in a Speed Vac, the gels were rehydrated in a minimal volume of trypsin solution (10 μg/mL in 40 mmol/L ammonium bicarbonate) and incubated at 37 °C overnight. The supernatant was directly applied onto the sample plate with equal amounts of matrix.

2.9. MALDI-TOF MS analysis and protein identification

Mass spectra were recorded on an Applied Biosystems 4700 Proteomics Analyzer (Framingham, MA, USA). The instrument was

set as reflector mode with 20 kV accelerating voltage. Laser shots at 5000 per spectrum were used to acquire the spectra with a mass range from 600 to 3000 Da. Data were processed using 4700 Explorer software. MASCOT was used to search for proteins in the NCBI database (http://www.ncbi.nlm.nih.gov/) using MS data. The search was restricted to one missed cleavage site and 0.1 Da error tolerance for MS/MS fragments. Protein modifications were performed including carboxyamidomethylation of cysteine and oxidation of methionine. Duplicate or triplicate runs were made to ensure the accuracy of the analysis.

2.10. Measurement of mitochondrial transmembrane potential

Mitochondrial transmembrane potential ($\Delta\Psi_m$) was detected using a JC-1 mitochondrial membrane potential assay kit (Beyotime Biotech), following the manufacturer's protocol. After treatment, the cells were incubated at 37 °C for 20 min with 5 μg/mL JC-1, then washed twice with PBS and placed in fresh medium without serum. Flow cytometry was performed using a Beckman Coulter Altra flow cytometer (Beckman Coulter Inc., Fullerton, CA, USA) equipped with a single 488 nm argon laser. A minimum of 10,000 cells per sample was acquired and analyzed using WinMDI V2.8 software.

2.11. Measurement of oxidative stress

The levels of intracellular ROS were determined using a ROS assay kit (Beyotime Biotech) and performed following the manufacturer's protocol. Briefly, cells in 35 mm Petri dishes were incubated in RPM1640 medium containing 0.1 mmol/L $[YbCit_2]^{3-}$ for 24 h. The cells were harvested and incubated with 10 μmol/L DCFH-DA at room temperature for 30 min in the dark and then analyzed using a flow cytometer (Beckman Coulter Altra). The fluorescence intensity was monitored using an excitation wavelength of 488 nm and an emission wavelength of 525 nm.

2.12. Western blot analysis

Western blot analysis was performed using primary antibodies (Abs) against Bcl-2, Bax, VDAC1, VDAC2 and GAPDH (from Santa Cruz Biotechnology, Santa Cruz, CA, USA), PARP, SOD1 and Nm23 (from Bios), cleaved caspase-9 and eEF2 (from Abzoom, Dallas, TX, USA) at optimized dilutions. The apoptosis-related proteins, including Bcl-2, Bax, cleaved caspase-9 and 89 kDa cleaved PARP, Nm23, VADC1 and VADC2, were separated by 1D SDS-PAGE. Aliquots of 25 μg of total protein extracts were separated by electrophoresis in SDS polyacrylamide gels (10% or 12.5%). GAPDH was used for the normalization of each protein to ensure equal protein loading. Western blot analyses of the 2D gels were performed for the validation of altered SOD1 and eEF2 expression. Following the separation of SDS-PAGE or 2D gel electrophoresis, proteins were transferred to polyvinylidene fluoride (PVDF) membranes (Millipore, Madison, WI, USA). The blots were incubated overnight at 4 °C with the primary Ab. After three washes with TBS-Tween, blots were incubated for 1 h at 25 °C with the secondary Ab. After further washes, the immune complexes were revealed by enhanced chemiluminescence (Pierce ECL detection kit, Thermo Fisher Scientific Inc., Rockford, USA).

2.13. Statistical analysis

Statistical analysis was done using two-tailed Student's *t*-tests and $P < 0.05$ was considered significant. Data were expressed as the mean ± SD of triplicate samples and reproducibility was confirmed in at least two independent experiments.

3. Results

3.1. $[YbCit_2]^{3-}$-induced cell growth inhibition and apoptosis

The effects of $[YbCit_2]^{3-}$ on the proliferation and apoptosis of HeLa cells were investigated. Cells were treated with the indicated concentration of $[YbCit_2]^{3-}$ for 24 h and cell viability were determined by MTT assay. As shown in Fig. 1A, after treatment cell viability decreased significantly in a dose-dependent manner compared with the untreated control ($P < 0.05$). The IC_{50} value for $[YbCit_2]^{3-}$ on HeLa cells was 0.17 mmol/L. After treatment with 0.1 mmol/L $[YbCit_2]^{3-}$ for 12 or 24 h, cells were stained with Hoechst 33258 and visualized using fluorescent microscopy. Typical morphology of apoptosis was detected in $[YbCit_2]^{3-}$-treated HeLa cells. The percentage of apoptotic cells is 10 ± 1.32% and 27.67 ± 2.47% for the treated cells after 12 and 24 h treatment, respectively (Fig. 1B). In addition, flow cytometric analysis was performed to identify and quantify the apoptotic cells using Annexin V-FITC/PI staining. There was a significant increase in the percentage of apoptotic cells after $[YbCit_2]^{3-}$ treatment compared with the un-treated cells. The increase levels are 51.3 ± 0.99% and 74.35 ± 1.77%, respectively, for the treated cells after 12 and 24 h treatment (Fig. 1C).

3.2. Comparative proteomics of $[YbCit_2]^{3-}$-treated cells

The proteomes of control and $[YbCit_2]^{3-}$-treated cells were analyzed by 2DE. Representative 2D gel images are shown in Fig. 2A and detailed alternations in Fig. 2B. By applying a threshold of 2-fold variation, 12 spots were identified as being differentially expressed after $[YbCit_2]^{3-}$ treatment. Table 1 lists the differentially expressed proteins identified by peptide mass fingerprinting (PMF). The first group comprised proteins involved in apoptosis and cell proliferation. The expressed levels of human nucleoside diphosphate kinase B complex (Nm23) and tyrosine 3/tryptophan 5 mono-oxygenase activation protein were downregulated, whereas prohibitin (PHB) was upregulated. The second group of proteins was related to redox state, including superoxide dismutase 1 (SOD 1) and quinolinate phosphoribosyltransferase (QPRTase). The third group of proteins was associated with protein translation, degradation and biosynthesis, including the downregulation of eukaryotic translation elongation factor 2 (eEF2), ribosomal protein, large, P0 (RPLP0), eukaryotic translation initiation factor 3, subunit 2 beta (eIF3i) and the upregulation of proteasome beta 3 subunit.

3.3. Changes in mitochondrial transmembrane potential in $[YbCit_2]^{3-}$-treated cells

$\Delta\Psi_m$ was monitored using JC-1 staining. Fig. 3A shows representative JC-1 fluorescence in both FL-1 and FL-2 channels. The control cells displayed high red fluorescence (red in Fig. 3A) and weak green fluorescence (shown as blue in the Fig. 3A), indicating hyperpolarized mitochondria. However, cells treated with $[YbCit_2]^{3-}$ exhibited increased green fluorescence and decreased red fluorescence, suggesting the depolarization of mitochondria and reduced $\Delta\Psi_m$. The results also showed reduction of $\Delta\Psi_m$ upon incubation with $[YbCit_2]^{3-}$ (Fig. 3B). The ratio of cells with high membrane potential exposed to $[YbCit_2]^{3-}$ decreased from 79.65 ± 4.45% to 61.25 ± 6.29% after 24 h treatment ($P < 0.05$).

3.4. ROS generation in $[YbCit2]^3$-treated cells

As shown in Fig. 4, after incubation of Hell cells with $[YbCit_2]^{3-}$ (0.1 mmol/L) for 24 h, intracellular ROS generation increased significantly ($P < 0.05$). The level of ROS in $[YbCit_2]^{3-}$-treated cells was

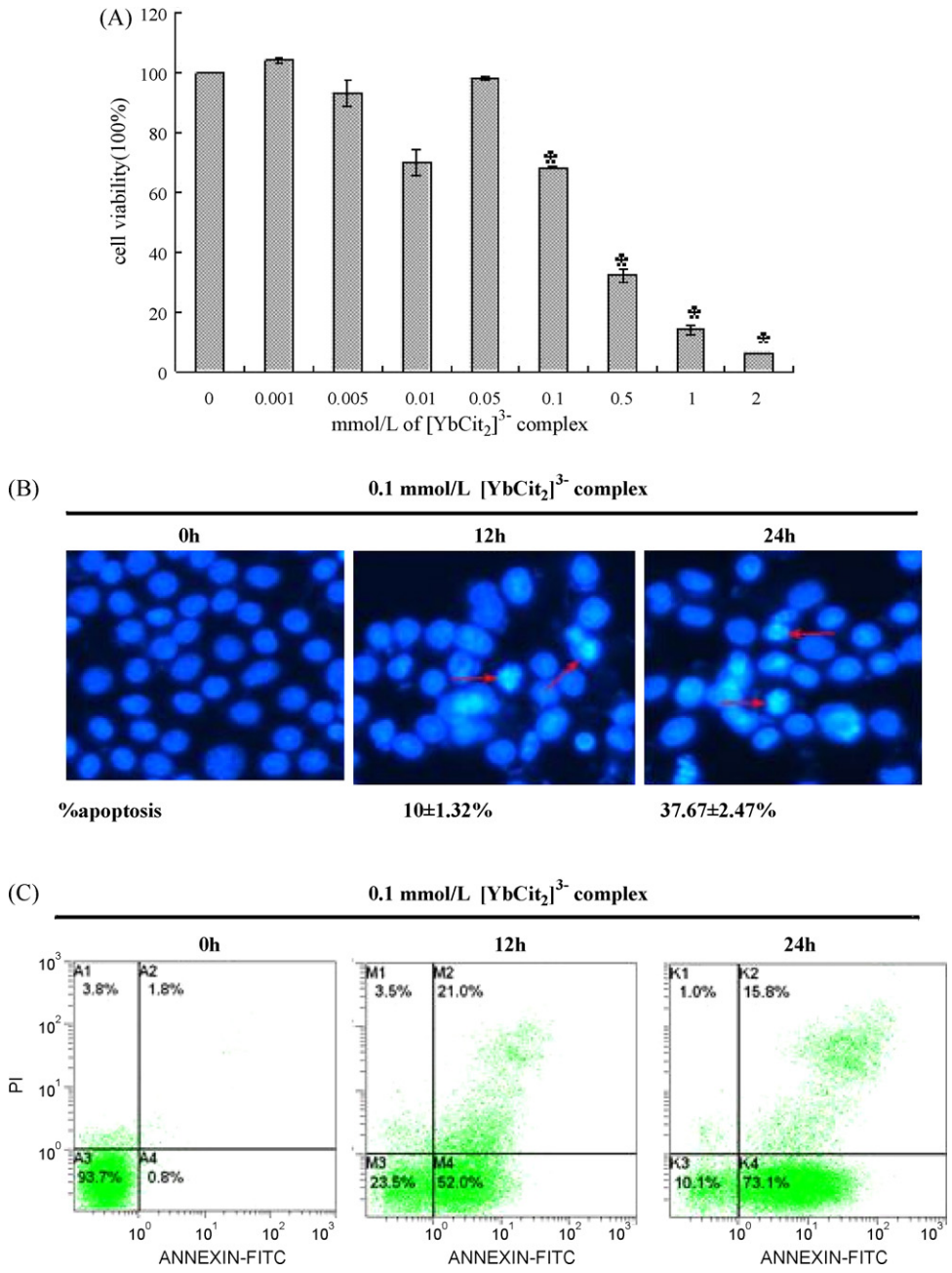

Fig. 1. Effects of $[YbCit_2]^{3-}$ on the proliferation and apoptosis of HeLa cells. (A) Effects of different concentrations of $[YbCit_2]^{3-}$ on cell viability. (B) Hoechst 33258-staining of HeLa cells treated with $[YbCit_2]^{3-}$ (*$P < 0.05$). Red arrows indicate several apoptotic cells with typical condensation of chromatin. The apoptosis rate could not be read for 0 h. (C) Annexin V-FITC/PI staining flow cytometry analysis of the rate of apoptosis rate in HeLa cells treated with $[YbCit_2]^{3-}$. A, M, K represented different samples obtained after 0, 12, and 24 h treatment with $[YbCit_2]^{3-}$, respectively. The four parts separated in A, or M, or K represent different types of cells, i.e., A1, M1, K1 represent for damaged cells (AxV-FITC−/PI+); A2, M2, K2 for late apoptotic/necrotic cells (AxV-FITC+/PI+); A3, M3, k3 for live cells (AxV-FITC−/PI−); A4, M4, K4 for early apoptotic cells (AxV-FITC+/PI−). The figures shown here are representative data of triplicate experiments. (For interpretation of the references to color in this figure legend, the reader is referred to the web version of the article.)

3.40-fold higher than the level of ROS in control cells throughout the experiment.

3.5. Western blot analysis

Western blot analysis was performed to detect any changes in the levels of apoptosis-related proteins, including the proapoptotic protein Bax, the antiapoptotic protein Bcl-2 and the downstream elements caspase-9 and PARP. Fig. 5A shows that Bax expression was upregulated and Bcl-2 was downregulated after treatment with $[YbCit_2]^{3-}$ at 0.1 mmol/L for 24 h. The ratio of Bax/Bcl-2 was significantly increased compared with the controls. Cleaved caspase-9 and the inactive form of the 89-kDa fragment of cleaved PARP were detected. These data suggest that the mitochondrial apoptosis pathway was involved in $[YbCit_2]^{3-}$-induced cell apoptosis.

Western blot analysis was also used to confirm the altered expressions of proteins in response to $[YbCit_2]^{3-}$ treatment (Fig. 5B). The proteins of eEF2 and SOD1 were downregulated in $[YbCit_2]^{3-}$-induced cells compared with controls. The altered expression levels of these proteins matched well with the proteins differentially expressed in 2DE. The proteomics result showed that human nucleoside diphosphate kinase B complex was downregulated. To confirm this result, western blot analysis was performed using primary antibodies against Nm23. Results showed that the

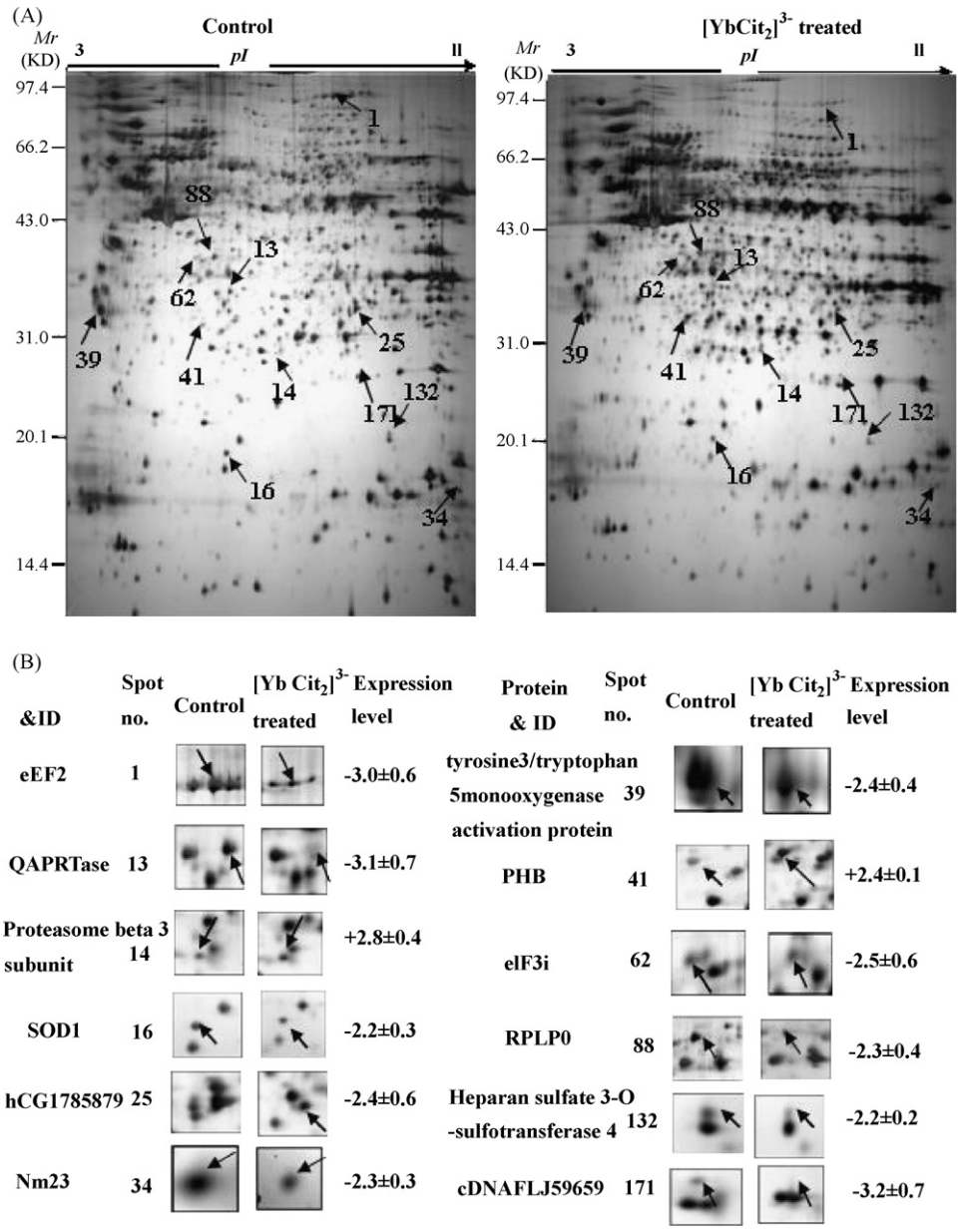

(B)

Spot no.	&ID	Control	[Yb Cit$_2$]$^{3-}$ treated	Expression level	Spot no.	Protein & ID	Control	[Yb Cit$_2$]$^{3-}$ treated	Expression level
1	eEF2			-3.0±0.6	39	tyrosine3/tryptophan 5monooxygenase activation protein			-2.4±0.4
13	QAPRTase			-3.1±0.7	41	PHB			+2.4±0.1
14	Proteasome beta 3 subunit			+2.8±0.4	62	eIF3i			-2.5±0.6
16	SOD1			-2.2±0.3	88	RPLP0			-2.3±0.4
25	hCG1785879			-2.4±0.6	132	Heparan sulfate 3-O -sulfotransferase 4			-2.2±0.2
34	Nm23			-2.3±0.3	171	cDNAFLJ59659			-3.2±0.7

Fig. 2. Representative 2D gel images of HeLa cells. (A) HeLa cells treated with or without 0.1 mmol/L [YbCit$_2$]$^{3-}$ in FBS-free culture medium for 24 h followed by 2D analysis. Arrows indicate proteins whose expressions were altered and identified by peptide mass fingerprinting. Spot numbers correspond to those listed in the first column of Table 1. (B) Detailed alternation of identified protein spots.

expression of Nm23 was significantly decreased (Fig. 5A). Voltage-dependent anion-selective channel (VDAC) has been recognized as a key protein in mitochondrial-mediated apoptosis [15]. The proteins VDAC1 and VDAC2 were also investigated in this study. However, VDAC1 (Fig. 5A) showed no obvious changes and VDAC2 was not detected (results not shown).

4. Discussion

In this study, ytterbium was chosen as a representative heavy Ln to be investigated on its cytotoxic activity against HeLa cells. After [YbCit$_2$]$^{3-}$-treatment, the growth of HeLa cells was inhibited and typical morphological changes were detected relating to apoptosis. Flow cytometry revealed an increase in the apoptotic cell rate in response to [YbCit$_2$]$^{3-}$-treatment. These data suggested that [YbCit$_2$]$^{3-}$ significantly induced the inhibition of cell growth and promoted apoptosis in HeLa cells.

Corresponding to the proteomic changes of mitochondrial proteins and oxidative stress-related proteins, $\Delta\Psi_m$ and ROS were further measured to study the mechanism of apoptosis caused by [YbCit$_2$]$^{3-}$. The obtained data showed that [YbCit$_2$]$^{3-}$ resulted in a decrease in $\Delta\Psi_m$ and the generation of ROS, which is consistent with a previous report [8] and our previous results on [LaCit$_2$]$^{3-}$-induced apoptosis. Generally, apoptotic stimuli induce the opening of membrane permeability transition pores (PTP) followed by the release of proapoptotic proteins from the mitochondrial intermembranous space [15,16]. Activation of caspase-9 and 89-kDa cleaved PARP were also detected. The expression level of proapoptotic protein Bax was increased while the antiapoptotic protein Bcl-2 was decreased, suggesting that mitochondrial permeability is mediated through the proteins of Bcl-2 family in [YbCit$_2$]$^{3-}$-treated HeLa cells. Similar to the effect of [LaCit$_2$]$^{3-}$ on HeLa cells, an intrinsic apoptosis pathway could also be involved in [YbCit$_2$]$^{3-}$-induced cytotoxicity.

Table 1
Proteins and their alterations after $[YbCit_2]^{3-}$ treatment (0.1 mmol/L for 24 h).

Spot no.	Protein ID	NCBI accession no.	MW (kDa)/pI	Reported function	Expression level[a]	Peptides matched[b]
1	Elongation factor 2 (eEF2)	4503483	95.3/6.41	Translation	−3.0 ± 0.6	15
13	Quinolinate phosphoribosyltransferase (QAPRTase)	13477197	31.1/5.81	Oxidation reduction	−3.1 ± 0.7	8
14	Proteasome beta 3 subunit	22538465	23.2/6.14	Protein degradation	+2.8 ± 0.4	9
16	Superoxide dismutase 1. soluble (SOD1)	4507149	16.1/5.7	Oxidation reduction	−2.2 ± 0.3	6
25	hCG1785879	119602242	10.8/11.31	Unclear	−2.4 ± 0.6	6
34	Nm23 human nucleoside diphosphate kinase B complexed (Nm23)	1421609	17.1/8.55	Apoptosis	−2.3 ± 0.3	8
39	Tyrosine 3/tryptophan 5 mono-oxygenase activation protein, epsilon polypeptide.	5803225	29.1/4.63	Signal transduction	−2.4 ± 0.4	12
41	Prohibitin (PHB)	4505773	29.8/5.57	Apoptosis	+2.4 ± 0.1	7
62	Eukaryotic translation initiation factor 3, subunit 2 beta (eIF3i)	4503513	36.5/5.38	Protein biosynthesis	−2.5 ± 0.6	7
88	Ribosomal protein, large, PO (EPLPO)	12654583	34.2/5.42	Translation	−2.3 ± 0.4	9
132	Heparan sulfate 3-O-sulfotransferase 4	126140598	15.6/9.58	Metabolic process	−2.2 ± 0.2	4
171	cDNAFLJ59659, highly similar to vinculin	194388374	100.8/5.35	Cell adhesion	−3.2 ± 0.7	13

[a] Expression level: trends of protein expression in $[YbCit_2]^{3-}$ treated Hela cells when compared with the control. + represents an increase of protein, while − represents a decrease in protein expression.
[b] Peptides matched by mass fingerprinting.

Mitochondria respond to an apoptotic signal by opening the mitochondrial PTP. PTP is composed of VDAC, outer mitochondrial membrane (OMM), adenine nucleotide translocase (ANT) and cyclophilin D. VDAC plays a key role in the regulation of mitochondrial-mediated apoptosis. All proteins in the VDAC family, including three isoforms VDAC1, VDAC2 and VDAC3, are located on the mitochondrial outer membrane [17]. In this study, VDAC2 expression in HeLa cells was not detected by western blot analysis (results not shown), while VDAC1 expression was observed to be unchanged after $[YbCit_2]^{3-}$-treatment. Those results imply that VDAC expression might not play a key role in the process of $[YbCit_2]^{3-}$-induced apoptosis in HeLa cells. On the other hand, Ca^{2+} overload induces PTP opening and appears to cause both apoptotic and necrotic cell death [18]. Ln ions, as analogs of Ca^{2+} [19], could directly bind to divalent metal binding sites on the outer side of mitochondrial PTP, thus induce its opening or closing. Ln ions might also prevent mitochondrial membrane permeability transition, as Ln ions inhibit the accumulation of Ca^{2+} by mitochondria [20]. As reported, La^{3+} displays a dual profile of effects towards mitochondria depending on the concentration used. Exposure to La^{3+} at 10–100 nmol/L induced permanent swelling of mitochondria, dissipation of membrane potential, ROS production, lipid peroxidation and release of cytochrome *c* [21]. However, La^{3+} at a higher concentration induces VDAC channel closure when assayed in single or multichannel studies [22,23]. Here we showed that $[YbCit_2]^{3-}$ is analogous to $[LaCit_2]^{3-}$ in that it functions as a 'super calcium' within mitochondria, rather than as a calcium antagonist in the progress of $[YbCit_2]^{3-}$-induced apoptosis of HeLa cells.

ROS also play important roles in the induction of cell apoptosis under both physiological and pathological conditions. Mitochondria are both the source and target of ROS [24]. In this paper, ROS levels were found to be significantly higher in HeLa cells after 24 h treatment with $[YbCit_2]^{3-}$, which suggests that ROS could be another important factor associated with $[YbCit_2]^{3-}$-induced apoptosis. This is also consistent with the previous report [8] and our results from $[LaCit_2]^{3-}$. Accordantly, the proteomic results

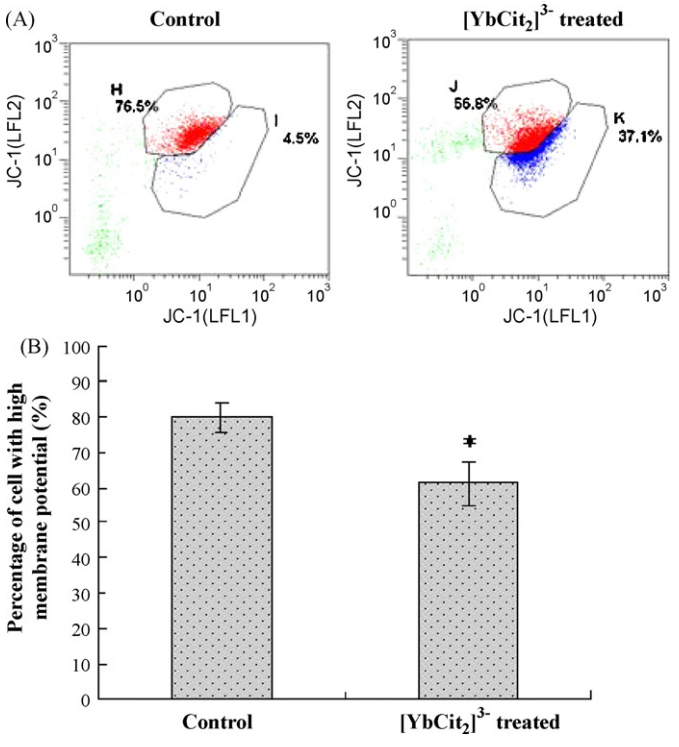

Fig. 3. Cytofluorimetric analysis of mitochondrial membrane potential ($\Delta\Psi_m$) by JC-1 staining. HeLa cells exposed to 0.1 mmol/L $[YbCit_2]^{3-}$ for 24 h were analyzed and compared with control cells. (A) One representative profile out of three replicates. Cells with high $\Delta\Psi_m$ are indicated in red and those with low $\Delta\Psi_m$ in blue; numbers refer to the percentage of cells. (B) Percentage of cells with high $\Delta\Psi_m$ (%). Each point represents the mean ± SD of three replicates (*$P < 0.05$). (For interpretation of the references to color in this figure legend, the reader is referred to the web version of the article.)

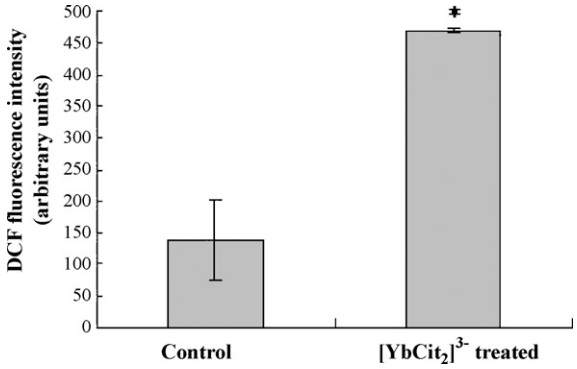

Fig. 4. $[YbCit_2]^{3-}$-induced the generation of ROS in HeLa cells. HeLa cells were pretreated with 0.1 mmol/L $[YbCit_2]^{3-}$ (FBS free) for 24 h and incubated with 10 mmol/L DCFH-DA for 30 min at 37 °C (see methodology). The fluorescent intensity of DCFH was measured using flow cytometry (*$P < 0.05$).

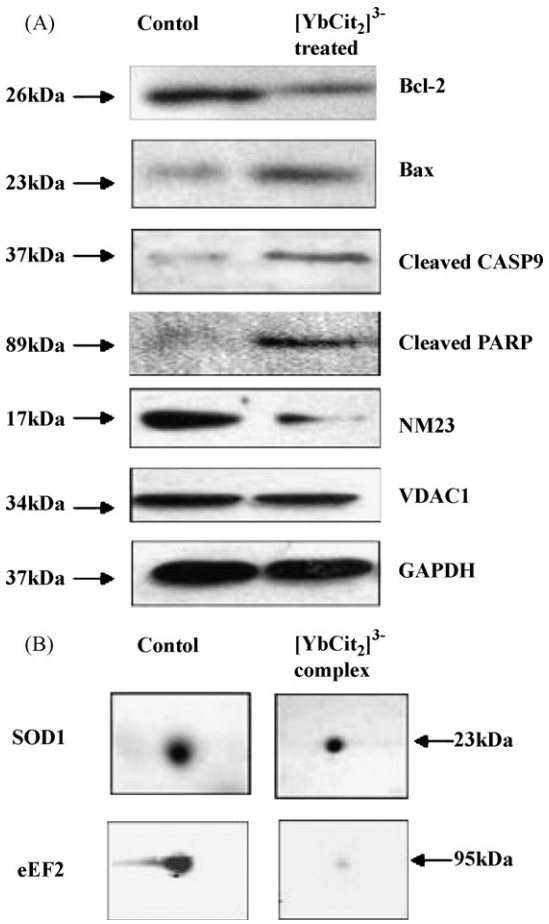

Fig. 5. The $[YbCit_2]^{3-}$-sensitive proteins in HeLa cells identified by western blot analyses. (A) Western blot analyses of apoptosis-related proteins separated by SDS-PAGE. GAPDH was used as an internal control. (B) Western blot analysis of two proteins separated by 2D-GE. This is a representative result from three independent experiments.

revealed profound alternations in proteins relating to oxidative and stress response, i.e., SOD1 and quinolinate phosphoribosyltransferase (QPRTase) were significantly downregulated. SOD1 is a major defense enzyme against ROS by detoxifying the superoxide anion. RNA interference against SOD1 induces HeLa cell death rather than senescence [25]. Mammalian QPRTase is a key enzyme in the catabolism of quinolinate, an intermediate in the process of tryptophan to nicotinamide adenine dinucleotide (NAD) [26]. As a carrier of active caspases, it is also an essential factor in apoptosis [27]. Inhibition of NAD synthesis using FK-866-induced apoptosis in human leukemia and hepatocarcinoma cells, and in various types of tumor xenografts [28]. NAD and NADP are fundamental mediators of various biological processes, including energy metabolism, mitochondrial functions, calcium homeostasis, anti-oxidation, oxidative-stresses generation, and cell death. Mitochondrial NADH-dependent ROS generation and NADPH oxidase-dependent ROS generation are two critical mechanisms of ROS generation [29]. Thus the downregulated expression of SOD1 and QPRTase could be two major reasons for the increase of ROS in $[YbCit_2]^{3-}$-treated HeLa cells.

Protein synthesis can be subdivided conveniently into three phases: initiation, elongation and termination [30]. During apoptosis there is a considerable and rapid reduction in the global rate of protein synthesis [31,32]. A recent study indicated that inhibition of protein translation activated the mitochondrial pathway of apoptosis because of the degradation of one or more anti-apoptotic proteins *via* proteasomes. The antiapoptotic Bcl-2 family protein myeloid cell leukemia-1 (Mcl-1) was identified as one such protein whose degradation triggered the apoptotic machinery [33]. Analogous to that report, upregulated Bax and downregulated Bcl-2 expressions were detected in this study when HeLa cells were treated with $[YbCit_2]^{3-}$, leading to a significant increase in the Bax/Bcl-2 ratio compared with the control. Those results imply that $[YbCit_2]^{3-}$ might induce the apoptosis of HeLa cells *via* the translation and proteasome related pathway. When compared with the effect of $[LaCit_2]^{3-}$ on HeLa cells, protein changes associated with their translation and degradation were also observed in $[YbCit_2]^{3-}$-treated cells, including decreased expression of eEF2, RPLP0 and eIF3i and increased expression of the proteasome beta 3 subunit. EIF3 plays a central role in binding the initiator methionyl-tRNA and mRNA with a 40S ribosomal subunit to initiate protein translation [34], regulating synthesis of a subpopulation of proteins, and thus playing a specific role in the control of cell growth [35]. EIF3 consists of 13 putative subunits, where its subunit 2 is named as eIF3i, also known as TRIP-1. EIF3i is a phosphorylation substrate of the transformation growth factor-type II (TGF-II) receptor, acting as a negative modulator of the TGF pathway [36]. Overexpression of eIF3i might cause uncontrolled cell growth and cancer by inhibiting TGF signaling [35]. The decreased eIF3i expression further confirmed the involvement of an apoptotic pathway relating to translation initiation and elongation and protein degradation in $[YbCit_2]^{3-}$-treated HeLa cells.

As reported, *Nm23* gene expression is strictly related to the state of cell growth, its antisense RNA-transfected cells show consistently slower proliferation activity than the control [37]. So far two human *Nm23* genes have been identified: *Nm23-H1* and *Nm23-H2*, coding for the A and B subunits of nucleoside diphosphate kinase (NDPK), respectively [38]. Similar to the effect of $[LaCit_2]^{3-}$, the Nm23 protein was also downregulated in $[YbCit_2]^{3-}$-treated HeLa cells, indicating the participation of Nm23 in the apoptosis.

HPV infection is linked with the development of cervical cancer. Short treatment of cells with Lns could block the RNA replication of flavivirus. Results in our paper showed that $[YbCit_2]^{3-}$ could induce the apoptosis of cervical cancer cells HeLa after 12 or 24 h treatment. Together with our results on $[LaCit_2]^{3-}$, it is reasonable to propose that Lns could possibly be developed as a drug for therapy in patient with cervical cancer through both inhibiting the replication of HPV and inducing the apoptosis of cancer cells.

In conclusion, $[YbCit_2]^{3-}$-induced significant growth inhibition and apoptosis in human cervical cancer cells HeLa. Using a proteomics strategy, 12 proteins were identified as being expressed differentially. Most of them are associated with cell apoptosis or proliferation, redox-state regulation, and protein translation or degradation. Among these proteins, SOD1 and eEF2 were further validated using western blot analysis. In addition, $[YbCit_2]^{3-}$ treatment also induced a decrease in $\Delta\Psi_m$ and an increase in ROS generation. An increase in the ratio of Bax/Bcl-2 and activation of the downstream apoptotic factors caspase-9 and 89-kDa cleaved PARP were involved in $[YbCit_2]^{3-}$-induced apoptosis. Those results indicate that mitochondria is involved in the major apoptotic pathway triggered by $[YbCit_2]^{3-}$ in HeLa cells, analogous to the apoptosis-induced mechanism of $[LaCit_2]^{3-}$. Those results imply that Lns might generally induce the apoptosis of tumor cells through the mitochondrial pathway.

Conflict of interest statement

The authors declare that there are no conflicts of interest.

Acknowledgments

This work was supported by the National Natural Science Foundation of China (No. 20637010) and Shenzhen Bureau of Science,

Technology and Information. We thank Drs. Zhixiong Zhuang and Jianjun Liu (Shenzhen Municipal Center for Disease Control and Prevention, PR China) for their kind help in the experiments.

Appendix A. Supplementary data

Supplementary data associated with this article can be found, in the online version, at doi:10.1016/j.cbi.2009.07.013.

References

[1] S. Yu, J. Hu, X. Yang, K. Wang, Z.M. Qian, La^{3+}-induced extracellular signalregulated kinase (ERK) signaling *via* a metal-sensing mechanism linking proliferation and apoptosis in NIH 3T3 cells, Biochemistry 45 (2006) 1217–1225.
[2] S.I. Hashemy, J.S. Ungerstedt, F.Z. Avval, A. Holmgren, Motexafin gadolinium, a tumor-selective drug targeting thioredoxin reductase and ribonucleotide reductase, J. Biol. Chem. 281 (2006) 10691–10697.
[3] Y. Dai, J. Li, J. Li, L. Yu, G. Dai, A. Hu, L. Yuan, Z. Wen, Effects of rare earth compounds on growth and apoptosis of leukemic cell lines, In Vitro Cell. Dev. Biol. Anim. 38 (2002) 373–375.
[4] S. Yu, L. Yuan, X. Yang, K. Wang, Y. Ke, Z.M. Qian, La^{3+}-promoted proliferation is interconnected with apoptosis in NIH 3T3 cells, J. Cell. Biochem. 94 (2005) 508–519.
[5] X. Li, A. Zhou, W. Yu, X. Chen, Effect of lanthanum citrate on two cell lines: human lung cancer cells PG and human gastric carcinoma cells BGC2823, J. Chin. Rare Earths Soc. 18 (2000) 156–159.
[6] I. Kostova, Lanthanides as anticancer agents, Curr. Med. Chem. Anticancer Agents 5 (2005) 591–602.
[7] T. Sato, M. Hashizume, Y. Hotta, Y. Okahata, Morphology and proliferation of B16 melanoma cells in the presence of lanthanoid and Al^{3+} ions, Biometals 11 (1998) 107–112.
[8] H. Liu, L. Yuan, X. Yang, K. Wang, La^{3+}, Gd^{3+}, and Yb^{3+} induced changes in mitochondrial structure, membrane permeability, cytochrome *c* release and intracellular ROS level, Chem. Biol. Interact. 146 (2003) 27–37.
[9] L.M. Shen, Z.Y. Lan, Q. Liu, J.Z. Ni, Apoptosis of cancer cells induced by lanthanum citrate, J. Chin. Rare Earths Soc. 27 (2009) 441–446.
[10] J.M. Walboomers, M.V. Jacobs, M.M. Manos, F.X. Bosch, J.A. Kummer, K.V. Shah, P.J. Snijders, J. Peto, C.J. Meijer, N. Muñoz, Human papillomavirus is a necessary cause of invasive cervical cancer worldwide, J. Pathol. 189 (1999) 12–19.
[11] M. Steben, E. Duarte-Franco, Human papillomavirus infection: epidemiology and pathophysiology, Gynecol. Oncol. 107 (2007) S2–5.
[12] G. Wengler, G. Wengler, A. Koschinski, A short treatment of cells with the lanthanide ions La^{3+}, Ce^{3+}, Pr^{3+} or Nd^{3+} changes the cellular chemistry into a state in which RNA replication of flaviviruses is specifically blocked without interference with host-cell multiplication, J. Gen. Virol. 88 (2007) 3018–3026.
[13] A. Görg, W. Weiss, M.J. Dunn, Current two-dimensional electrophoresis technology for proteomics, Proteomics 4 (2004) 3665–3685.
[14] H.J. Won, C.H. Han, Y.H. Kim, H.J. Kwon, B.W. Kim, J.S. Choi, K.H. Kim, Induction of apoptosis in human acute leukemia Jurkat T cells by Albizzia julibrissin extract is mediated *via* mitochondria-dependent caspase-3 activation, J. Ethnopharmacol. 106 (2006) 383–389.
[15] M. Crompton, The mitochondrial permeability transition pore and its role in cell death, Biochem. J. 341 (1999) 233–249.
[16] V. Gogvadze, J.D. Robertson, B. Zhivotovsky, S. Orrenius, Cytochrome *c* release occurs *via* Ca^{2+}-dependent and Ca^{2+}-independent mechanisms that are regulated by Bax, J. Biol. Chem. 276 (2001) 19066–19071.
[17] V. Shoshan-Barmatz, N. Keinan, H. Zaid, Uncovering the role of VDAC in the regulation of cell life and death, J. Bioenerg. Biomembr. 40 (2008) 183–191.
[18] Y. Tsujimoto, S. Shimizu, Role of the mitochondrial membrane permeability transition in cell death, Apoptosis 12 (2007) 835–840.
[19] J.Z. Ni, Bioinorganic Chemistry of Rare Earth Elements, Science Press, Beijing, 1995, pp. 13–59.
[20] L. Mela, Interactions of La^{3+} and local anesthetic drugs with mitochondrial Ca^{2+} and Mn^{2+} uptake, Arch. Biochem. Biophys. 123 (1968) 286–293.
[21] S. Dong, K. Wang, Calcium binding and translocation by the voltage-dependent anion channel: a possible regulatory mechanism in mitochondrial function, Thesis of Master Degree, National Research Laboratories of Natural and Biomimetic Drugs, Peking University Health Science Center, 2008.
[22] D. Gincel, H. Zaid, V. Shoshan-Barmatz, Calcium binding and translocation by the voltage-dependent anion channel: a possible regulatory mechanism in mitochondrial function, Biochem. J. 358 (2001) 147–155.
[23] V. Shoshan-Barmatz, D. Gincel, The voltage-dependent anion channel: characterization, modulation and role in mitochondrial function in cell life and death, Cell Biochem. Biophys. 39 (2003) 279–292.
[24] H.U. Simon, A. Haj-Yehia, F. Levi-Schaffer, Role of reactive oxygen species (ROS) in apoptosis induction, Apoptosis 5 (2000) 415–418.
[25] G. Blander, R.M. de Oliveira, C.M. Conboy, M. Haigis, L. Guarente, Superoxide dismutase 1 knock-down induces senescence in human fibroblasts, J. Biol. Chem. 278 (2003) 38966–38969.
[26] S.I. Fukuoka, C.M. Nyaruhucha, K. Shibata, Characterization and functional expression of the cDNA encoding human brain quinolinate phosphoribosyltransferase, Biochim. Biophys. Acta 1395 (1998) 192–201.
[27] N. Katunuma, K. Ishidoh, J. Sakurai, M. Oda, N. Kamemura, Reciprocal relationship between the apoptosis pathway mediated by executioner caspases and the physiological NAD synthesis pathway, Adv. Enzyme Regul. 48 (2008) 19–30.
[28] M.K. Kim, J.H. Lee, H. Kim, S.J. Park, S.H. Kim, G.B. Kang, Y.S. Lee, J.B. Kim, K.K. Kim, S.W. Suh, S.H. Eom, Crystal structure of visfatin/pre-B cell colony-enhancing factor 1/nicotinamide phosphoribosyltransferase, free and in complex with the anti-cancer agent FK-866, J. Mol. Biol. 362 (2006) 66–77.
[29] H.Y. Wei, NAD+/NADH and NADP+/NADPH in cellular functions and cell death: regulation and biological consequences, Antioxid. Redox Signal. 10 (2008) 179–207.
[30] M. Bushell, M. Stoneley, P. Sarnow, A.E. Willis, Translation inhibition during the induction of apoptosis: RNA or protein degradation, Biochem. Soc. Trans. 32 (2004) 606–610.
[31] M.J. Clemens, M. Bushell, S.J. Morley, Degradation of eukaryotic polypeptide chain initiation factor (eIF) 4G in response to induction of apoptosis in human lymphoma cell lines, Oncogene 17 (1998) 2921–2931.
[32] S.J. Morley, L. McKendrick, M. Bushell, Cleavage of translation initiation factor 4G (eIF4G) during anti-Fas IgM-induced apoptosis does not require signalling through the p38 mitogen-activated protein (MAP) kinase, FEBS Lett. 438 (1998) 41–48.
[33] J.H. Woo, J.H. Kim, Phosphorylation of eukaryotic elongation factor 2 can be regulated by phosphoinositide 3-Kinase in the early stages of myoblast differentiation, Mol. Cells 21 (2006) 294–301.
[34] K. Asano, H.P. Vornlocher, N.J. Richter-Cook, W.C. Merrick, A.G. Hinnebusch, J.W. Hershey, Structure of cDNAs encoding human eukaryotic initiation factor 3 subunits. Possible roles in RNA binding and macromolecular assembly, J. Biol. Chem. 272 (1997) 27042–27052.
[35] Z. Dong, J.T. Zhang, Initiation factor eIF3 and regulation of mRNA translation, cell growth and cancer, Crit. Rev. Oncol. Hematol. 59 (2006) 169–180.
[36] L. Choy, R. Derynck, The type II transforming growth factor (TGF)-beta receptor-interacting protein TRIP-1 acts as a modulator of the TGF-beta response, J. Biol. Chem. 273 (1998) 31455–31462.
[37] P.J. Srivatsa, W.A. Cliby, G.L. Keeney, V.J. Suman, W.S. Harmsen, S.C. Ziesmer, P.C. Roche, K.C. Podratz, Expression of nm23/nucleoside diphosphate kinase-A protein in endometrial carcinoma, Gynecol. Oncol. 66 (1997) 238–245.
[38] M.A. Caligo, G. Cipollini, L. Fiore, S. Calvo, F. Basolo, P. Collecchi, F. Ciardiello, S. Pepe, M. Petrini, G. Bevilacqua, *NM23* gene expression correlates with cell growth rate and S-phase, Int. J. Cancer 60 (1995) 837–842.